

A symmetric BEM approach to strain gradient elasticity for 2D static boundary-value problems

Panzeca T¹, Terravecchia S.² and Polizzotto C³

¹ DICAM, Viale delle Scienze, 90128 Palermo, teotista.panzeca@unipa.it

² DICAM, Viale delle Scienze, 90128 Palermo, silvioterravecchia@gmail.com

³ DICAM, Viale delle Scienze, 90128 Palermo, castrenze.polizzotto@unipa.it

Keywords: Strain gradient elasticity, Symmetric Galerkin BEM.

Abstract. The symmetric Galerkin Boundary Element Method is used to address a class of strain gradient elastic materials featured by a free energy function of the (classical) strain and of its (first) gradient. With respect to the classical elasticity, additional response variables intervene, such as the normal derivative of the displacements on the boundary, and the work-conjugate double tractions. The fundamental solutions - featuring a fourth order partial differential equations (PDEs) system - exhibit singularities which in 2D may be of the order $1/r^4$.

New techniques are developed, which allow the elimination of most of the latter singularities.

The present paper has to be intended as a research communication wherein a part of the results, being elaborated within a more general paper [1], are reported.

Introduction

After the pioneering work of Mindlin [2], theories of strain gradient elasticity have become very popular, particularly within the domain of nano-technologies, that is, for problems where the ratio surface/volume tends to become very large and there is a need to introduce at least one internal length.

However the model introduced by Mindlin and then improved by Mindlin et al. [3] and Wu [4] leads to an excessive number of material coefficients, which at the best for isotropic materials reduce to the number of seven. In the early 1990's, Aifantis [5] introduced a signified material model of strain gradient elasticity which requires only three material coefficients, that is, the Lamé constants and one length scale parameter. The latter model was then developed further following the so-called Form II format given by Mindlin et al. [3], that is a theory centered on the existence of a free energy function of the (classical) strain and of its first gradient, which leads to the generation of symmetric stress fields (see Askes et al. [6] for historical details about the latter formulations and its applications).

Formulations in the boundary element method based on the strain gradient elasticity were pioneered by Polyzos et al. [7], Karlis et al. [8], who provide a collocation BEM formulation where the simplified constitutive equation by Aifantis [5], has been adopted. In latter papers only the fundamental solutions used in the collocation approach to BEM are provided.

In the case of the symmetric formulation of the BEM, Somigliana Identities (SIs) for the tractions and for the double tractions are also needed. These new SIs are necessary in order to get, through the process of modeling and weighing, a solving equation system having symmetric operators. In Polizzotto et al. [1] all the set of fundamental solutions is derived starting from the displacement fundamental solution given in [7,8].

The symmetric formulation is motivated by the high efficiency achieved within classical elasticity by the method in [9] with regard to the techniques used to eliminate the singularities of the fundamental solutions, the evaluation of the coefficients of the solving system and the computational procedures characterized by great implementation simplicity. This has already led to the birth of the computer code Karnak sGbem [10] operating in the classical elasticity.

The objective of this paper is to experiment new techniques and procedures that, applied in the context of strain gradient elastic materials, may permit one to obtain the related solving system.

1. Basic relations in 2D

The class of strain gradient elastic materials herein considered is featured by the following strain elastic energy

$$W = \frac{1}{2} \boldsymbol{\varepsilon} : \mathbf{E} : \boldsymbol{\varepsilon} + \frac{\ell^2}{2} \mathbf{E} :: [(\nabla \boldsymbol{\varepsilon})^T \cdot \nabla \boldsymbol{\varepsilon}] \quad (1)$$

that is a function of the 2nd order strains $\boldsymbol{\varepsilon}$ and of the strain gradient where ℓ is the internal length and $\boldsymbol{\varepsilon} = (\nabla \mathbf{u})_s$.

Eq.(1) provides the "primitive" stresses

$$\boldsymbol{\sigma}^{(0)} = \mathbf{E} \boldsymbol{\varepsilon}; \quad \boldsymbol{\sigma}^{(1)} = \ell^2 \nabla^2 \boldsymbol{\sigma}^{(0)} \quad (3a,b)$$

where \mathbf{E} is the classic isotropic elasticity tensor.

By the principle of the virtual power, the indefinite equilibrium equation and the following boundary conditions prove to be

$$\nabla \cdot \boldsymbol{\sigma} + \mathbf{b} = \mathbf{0} \quad \text{in } \Omega, \quad \mathbf{t} = \bar{\mathbf{t}} \quad \text{on } \Gamma, \quad \mathbf{r} = \bar{\mathbf{r}} \quad \text{on } \Gamma, \quad \mathbf{p} = \bar{\mathbf{p}} \quad \text{on the corner P}, \quad (4a,b,c,d)$$

where the total stresses $\boldsymbol{\sigma}$, the tractions \mathbf{t} , the double tractions \mathbf{r} and the force at the corner P are so defined

$$\boldsymbol{\sigma} = \boldsymbol{\sigma}^{(0)} - \ell^2 \nabla^2 \boldsymbol{\sigma}^{(0)}, \quad \mathbf{t} = \mathbf{n} \cdot \boldsymbol{\sigma} - \nabla^C \cdot (\mathbf{n} \cdot \boldsymbol{\sigma}^{(1)}), \quad \mathbf{r} = \mathbf{nn} : \boldsymbol{\sigma}^{(1)}, \quad \mathbf{p} = \llbracket \mathbf{sn} : \boldsymbol{\sigma}^{(1)} \rrbracket. \quad (5a,b,c,d)$$

In eq.(5b), the symbol ∇^C denotes the "reduced tangent gradient" defined as $\nabla^C = \nabla^{(s)} + K\mathbf{n}$ with $K = -\nabla^{(s)} \cdot \mathbf{n}$ being the boundary curvature at the considered point and $\nabla^{(s)} = (\mathbf{I} - \mathbf{nn}) \cdot \nabla$ is the operator of the tangent gradient on the boundary having normal \mathbf{n} ; in eq.(5d) \mathbf{s} denotes a unit vector tangent to the two boundary portions convergent in the corner P and the brackets $\llbracket \bullet \rrbracket$ indicate that the enclosed quantity is the difference between the related values taken on two sides of the corner P. For a more exhaustive understanding of the jump $\llbracket \bullet \rrbracket$ to see [2].

The constitutive equation relating the total stress $\boldsymbol{\sigma}$ to the strain is

$$\boldsymbol{\sigma} = \mathbf{E} : (\boldsymbol{\varepsilon} - \ell^2 \nabla^2 \boldsymbol{\varepsilon}) \quad (6)$$

where $\boldsymbol{\varepsilon}$ is the classical strain.

2. The fundamental solutions.

The introduction of eq.(6) in (4a) valid in Ω_∞ allows to express the latter in terms of displacements only [7,8] and to determine the fundamental solution of the displacements that for 2D solids proves to be

$$\mathbf{G}_{uu} = \frac{1}{16\pi\mu(1-\nu)} \left[\begin{array}{l} \left\{ -2 + 4 \left[\frac{2\ell^2}{r^2} - K_2 \left(\frac{r}{\ell} \right) \right] \right\} \mathbf{I} - \\ \left\{ -2(3-4\nu) \left[\text{Log}[r] + K_0 \left(\frac{r}{\ell} \right) \right] + 2 \left[\frac{2\ell^2}{r^2} - K_2 \left(\frac{r}{\ell} \right) \right] \right\} \mathbf{r} \otimes \mathbf{r} \end{array} \right] \quad (7)$$

where $K_0(\bullet)$ and $K_2(\bullet)$ are Bessel functions of the second kind and of order 0 and 2, respectively, and $\mathbf{r} = \boldsymbol{\xi} - \mathbf{x}$ is the distance between effect $\boldsymbol{\xi}$ and cause \mathbf{x} points. One can note that the singularity of the fundamental solution \mathbf{G}_{uu} does not depend on \mathbf{r} . Indeed, by performing the limit $\mathbf{r} \rightarrow \mathbf{0}$ one obtains

$$\mathbf{G}_{uu}(\boldsymbol{\xi} = \mathbf{x}) = \frac{1}{16\pi\mu(1-\nu)} \left[-2(3-4\nu) [\ln(2\ell) - \gamma] + 1 \right] \cdot \mathbf{I} \quad (8)$$

where γ is the Euler constant. So the limit for $\boldsymbol{\xi} \rightarrow \mathbf{x}$ ($\mathbf{r} \rightarrow \mathbf{0}$) the fundamental solution for isotropic gradient elasticity shows singularity of type $\ln(\ell)$.

In eq.(7) the limit of \mathbf{G}_{uu} for $\ell \rightarrow 0$ gives the classic isotropic elasticity solution (Kelvin) with singularity of type $\ln(r)$.

By the fundamental solution \mathbf{G}_{uu} in (7), taking in account eqs.(5b,c,d) and using the well-known procedure given in [11], it is possible, by exploiting the known properties of symmetry of the fundamental solutions, to derive the entire tableau provided below.

		cause measured at \mathbf{x}						
		\mathbf{f}	$-\mathbf{u}$	\mathbf{r}	\mathbf{g}	\mathbf{f}_E	$-\mathbf{u}_E$	ϑ
effect evaluated at ξ	\mathbf{u}	\mathbf{G}_{uu}	\mathbf{G}_{ut}	\mathbf{G}_{ug}	\mathbf{G}_{ur}	$[[\mathbf{G}_{uv}]]$	$[[\mathbf{G}_{up}]]$	$\mathbf{G}_{u\sigma}$
	\mathbf{t}	\mathbf{G}_{tu}	\mathbf{G}_{tt}	\mathbf{G}_{tg}	\mathbf{G}_{tr}	$[[\mathbf{G}_{tv}]]$	$[[\mathbf{G}_{tp}]]$	$\mathbf{G}_{t\sigma}$
	\mathbf{g}	\mathbf{G}_{gu}	\mathbf{G}_{gt}	\mathbf{G}_{gg}	\mathbf{G}_{gr}	$[[\mathbf{G}_{gv}]]$	$[[\mathbf{G}_{gp}]]$	$\mathbf{G}_{g\sigma}$
	\mathbf{r}	\mathbf{G}_{ru}	\mathbf{G}_{rt}	\mathbf{G}_{rg}	\mathbf{G}_{rr}	$[[\mathbf{G}_{rv}]]$	$[[\mathbf{G}_{rp}]]$	$\mathbf{G}_{r\sigma}$
	\mathbf{v}_E	$[[\mathbf{G}_{vu}]]$	$[[\mathbf{G}_{vt}]]$	$[[\mathbf{G}_{vg}]]$	$[[\mathbf{G}_{vr}]]$	$[[[\mathbf{G}_{vv}]]]$	$[[[\mathbf{G}_{vp}]]]$	$[[\mathbf{G}_{v\sigma}]]$
	\mathbf{p}_E	$[[\mathbf{G}_{pu}]]$	$[[\mathbf{G}_{pt}]]$	$[[\mathbf{G}_{pg}]]$	$[[\mathbf{G}_{pr}]]$	$[[[\mathbf{G}_{pv}]]]$	$[[[\mathbf{G}_{pp}]]]$	$[[\mathbf{G}_{p\sigma}]]$
	σ	$\mathbf{G}_{\sigma u}$	$\mathbf{G}_{\sigma t}$	$\mathbf{G}_{\sigma g}$	$\mathbf{G}_{\sigma r}$	$[[\mathbf{G}_{\sigma v}]]$	$[[\mathbf{G}_{\sigma p}]]$	$\mathbf{G}_{\sigma\sigma}$

Table 1. Fundamentals solutions for strain gradient elasticity.

The fundamental solutions \mathbf{G}_{hk} of Table I are characterized by two subscripts: the first indicates the effect at ξ , i.e. displacement for $h=u$, traction for $h=t$, displacement normal derivative for $h=g$, double traction for $h=r$, corner displacement for $h=v$, corner force for $h=p$, stress for $h=\sigma$; whereas the second subscript indicates – through a work-conjugate rule – the cause applied at \mathbf{x} , i.e. a unit concentrated force for $k=u$, a unit surface relative displacement for $k=t$, a unit concentrated double force for $k=g$, a unit higher order surface distortion for $k=r$, a unit corner force for $k=v$, a unit corner displacement for $k=p$, a unit imposed strain for $k=\sigma$. To consider the way in which the fundamental solutions included in the single $[[\cdot]]$ and double $[[[\cdot]]]$ brackets to see [2].

While the fundamental solutions represent the response in a point of the unlimited domain, the response to the distributed actions is provided by the SIs that in [1] are obtained by a generalization of the Betti theorem for the gradient elastic materials.

3. A case study.

The fundamental solutions present in the Table I show various orders of singularity, up to $1/r^4$ in the column related to $-\mathbf{u}$, up to $1/r^3$ in that related to $-\mathbf{u}_E$; furthermore the singularities present in the column $-\mathbf{u}_E$ present an order lower than that of $-\mathbf{u}$, relatively to the same effect.

In order to investigate the techniques useful to remove the singularities from the blocks of coefficients, a simple application in two-dimensional space is shown, but at this stage involving the study of fundamental solutions having the maximum order of singularity equal to $1/r^2$; it has to be remembered that in the symmetric BEM the coefficients are obtained by a double integration, the first (inner) regarding the modeling of the cause through appropriate shape functions and the second (external) regarding the effect weighed through shape functions, but dual in the energetic sense.

For this purpose, the example shown concerns a plate completely constrained on the boundary, subjected to the simple distortions $-\bar{\mathbf{u}}$, $-\bar{\mathbf{u}}_E$ and distortions of higher order $\bar{\mathbf{g}} = -\partial\bar{\mathbf{u}}/\partial n$.

The greater difficulties consist in removing the singularities when the cause is focused at the corner. But the simple observation that the vector $-\bar{\mathbf{u}}$ regards all the nodes of the boundary, including the vector $-\bar{\mathbf{u}}_E$ at the corner, allows to eliminate the higher order singularities after the first integration and, successively summing the effects, those remaining through the second integration.

The singularities present in the fundamental solutions used in the plate require shape functions of type $C^{(0)}$. This example is also used to develop the techniques of rigid motion that could be used in other applications to compute the coefficient blocks in which the techniques available are not sufficient to suppress the residual singularities.

The field response is derived by the SIs after the solution being obtained.

Let us analyze the two-dimensional plate of Fig.1 having the following physical and mechanical characteristics: $E = 1$, $\nu = 0.3$, $g = 0.1$, $s = 1$.

The plate is subjected to a linear displacement distribution $-\bar{\mathbf{u}}$, including the nodal displacement $-\bar{\mathbf{u}}_E$, and to the linear displacement normal derivatives $\bar{\mathbf{g}} = -\partial\bar{\mathbf{u}} / \partial n$, all imposed on the boundary (Fig.1c,d).

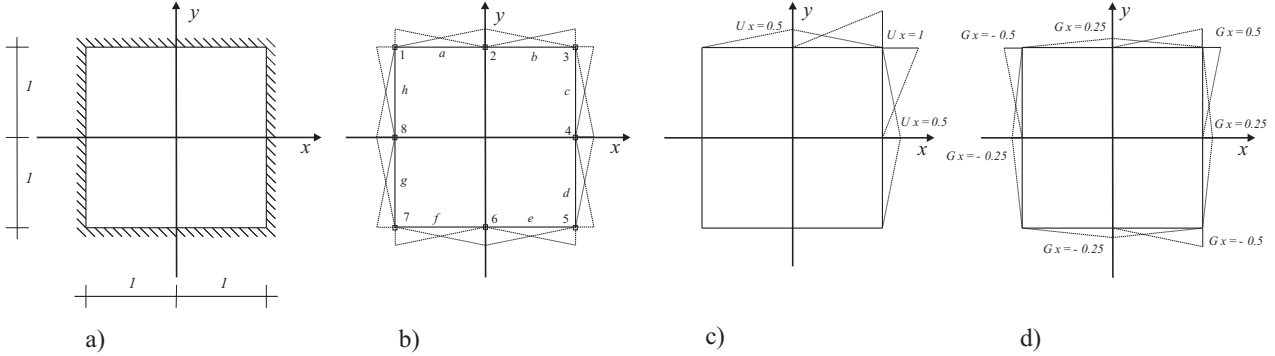


Fig.1 Plate: a) geometry and constraints; b) discretization into boundary elements and linear modelling of the boundary quantities; c) modelling of the displacements imposed; d) modelling of the displacement gradients imposed.

The displacement and displacement gradient fields imposed on the boundary are shown in Fig.1c,d.

The displacements imposed on the boundary are obtained by displacement field which is not the solution of the problem, but is able to define the nodal values U_x on the boundary of the plate

$$u_x = \frac{(1+x)(1+y)}{4} \quad (9a)$$

and as a consequence to obtain a normal derivative field

$$g_x = \frac{\partial u_x}{\partial n} = n_x \left[\frac{(1+y)}{4} \right] + n_y \left[\frac{(1+x)}{4} \right]. \quad (9b)$$

The two previous relations have been used to evaluate the nodal values of the displacements U_x and of the displacement derivatives G_x , as in Fig.1c,d.

For the plate of Fig.1a the boundary conditions are

$$\mathbf{u} = \bar{\mathbf{u}} \text{ on } \Gamma_u \quad \mathbf{g} = \bar{\mathbf{g}} \text{ on } \Gamma_g \quad \text{with } \Gamma_u \equiv \Gamma_g \quad (10a,b)$$

Let us proceed to write the SIs on the boundary following the compact notation proposed by Panzeca et al. [9]:

$$\mathbf{u} = \mathbf{u}[\mathbf{f}, \mathbf{r}] + \mathbf{u}[-\bar{\mathbf{u}}^{CPV}] + \mathbf{u}[-\bar{\mathbf{u}}_E] + \mathbf{u}[\bar{\mathbf{g}}] + \frac{1}{2}\bar{\mathbf{u}} \quad \text{on } \Gamma_u \quad (11a)$$

$$\mathbf{g} = \mathbf{g}[\mathbf{f}, \mathbf{r}] + \mathbf{g}[-\bar{\mathbf{u}}] + \mathbf{g}[-\bar{\mathbf{u}}_E] + \mathbf{u}[\bar{\mathbf{g}}^{CPV}] + \frac{1}{2}\bar{\mathbf{g}} \quad \text{on } \Gamma_g \quad (11b)$$

In the SIs:

- the superscripts are known quantities;
- the apex CPV indicates that the corresponding integral is evaluated as Cauchy Principal Value to which the related free term is added;
- $-\bar{\mathbf{u}}_E$ is a vector containing only the displacement of the corner;
- $\mathbf{u}[-\bar{\mathbf{u}}_E]$ and $\mathbf{g}[\bar{\mathbf{g}}^{CPV}]$ are, respectively, the displacement and normal derivative of displacement distribution on the boundary, computed as the difference between the response to the values of displacement imposed on the two portions of boundary afferent to the corner.

Introducing the latter SIs given in eqs.(11a,b) into the boundary conditions eqs.(10a,b) one has:

$$\mathbf{u}[\mathbf{f}, \mathbf{r}] + \mathbf{u}[-\bar{\mathbf{u}}^{CPV}] + \mathbf{u}[-\bar{\mathbf{u}}_E] + \mathbf{u}[\bar{\mathbf{g}}] - \frac{1}{2}\bar{\mathbf{u}} = \mathbf{0} \quad \text{on } \Gamma_u \quad (12a)$$

$$\mathbf{g}[\mathbf{f}, \mathbf{r}] + \mathbf{g}[-\bar{\mathbf{u}}] + \mathbf{g}[-\bar{\mathbf{u}}_E] + \mathbf{u}[\bar{\mathbf{g}}^{CPV}] - \frac{1}{2}\bar{\mathbf{g}} = \mathbf{0} \quad \text{on } \Gamma_g \quad (12b)$$

Let us now discretize the plate boundary into boundary elements (Fig.1b) and introduce the modeling of the quantities on the boundary (Fig.1c) as functions of the nodal variables through suitable matrices of shape functions \mathbf{N}_h , with $h = f, r, u, g$

$$\mathbf{f} = \mathbf{N}_f \mathbf{F}; \quad \mathbf{r} = \mathbf{N}_r \mathbf{R}; \quad \bar{\mathbf{u}} = \mathbf{N}_u \bar{\mathbf{U}}; \quad \bar{\mathbf{g}} = \mathbf{N}_g \bar{\mathbf{G}}. \quad (13a,b,c,d)$$

Since the vector $-\bar{\mathbf{u}}_E$ collects quantities to not be modeled, the following identity may be imposed

$$\bar{\mathbf{u}}_E = \bar{\mathbf{U}}_E. \quad (14)$$

In eqs.(13a-d) the quantities \mathbf{F} , \mathbf{R} , $\bar{\mathbf{U}}$, $\bar{\mathbf{G}}$ have the meaning of nodal quantities and precisely: force and double traction as unknowns, displacements and normal derivative of displacements as known quantities. To evaluate the vector $\bar{\mathbf{G}}$, because the discontinuity of the normal derivative at the corner P, a double node belonging respectively to the two portions of boundary afferent to P has to be considered.

Introducing the modeling (13a-d) and the relation (14) into eqs.(12a,b) and performing the weighing second Galerkin, using the shape functions in dual form, the following system in compact form is obtained as in Panzeca et al.[9]

$$\begin{bmatrix} \mathbf{A}_{uu} & \mathbf{A}_{ug} \\ \mathbf{A}_{gu} & \mathbf{A}_{gu} \end{bmatrix} \cdot \begin{bmatrix} \mathbf{F} \\ \mathbf{R} \end{bmatrix} + \begin{bmatrix} \mathbf{A}_{ut} + \mathbf{C}_{ut} & \mathbf{A}_{ur} \\ \mathbf{A}_{gt} & \mathbf{A}_{gr} + \mathbf{C}_{gr} \end{bmatrix} \cdot \begin{bmatrix} -\bar{\mathbf{U}} \\ \bar{\mathbf{G}} \end{bmatrix} + \begin{bmatrix} \llbracket \mathbf{a}_{up} \rrbracket \\ \llbracket \mathbf{a}_{gp} \rrbracket \end{bmatrix} (-\bar{\mathbf{U}}_E) = \begin{bmatrix} \mathbf{0} \\ \mathbf{0} \end{bmatrix} \quad (15)$$

Since some components of the vector $-\bar{\mathbf{U}}$ and of the vector $-\bar{\mathbf{U}}_E$ coincide, it is opportune to introduce the following relation

$$\bar{\mathbf{U}}_E = \mathbf{H}_E \bar{\mathbf{U}} \quad (16)$$

where the low rectangular matrix \mathbf{H}_E is a topological matrix made by $\mathbf{I}_{2 \times 2}$ and $\mathbf{0}_{2 \times 2}$ blocks.

The previous relation can be rewritten

$$\begin{bmatrix} \mathbf{A}_{uu} & \mathbf{A}_{ug} \\ \mathbf{A}_{gu} & \mathbf{A}_{gu} \end{bmatrix} \cdot \begin{bmatrix} \mathbf{F} \\ \mathbf{R} \end{bmatrix} + \begin{bmatrix} (\mathbf{A}_{ut} + \mathbf{C}_{ut}) + \llbracket \mathbf{a}_{up} \rrbracket^* \\ \mathbf{A}_{gt} + \llbracket \mathbf{a}_{gp} \rrbracket^* \end{bmatrix} \cdot (-\bar{\mathbf{U}}) + \begin{bmatrix} \mathbf{A}_{ur} \\ \mathbf{A}_{gr} + \mathbf{C}_{gr} \end{bmatrix} \cdot (\bar{\mathbf{G}}) = \begin{bmatrix} \mathbf{0} \\ \mathbf{0} \end{bmatrix} \quad (17)$$

where

$$\llbracket \mathbf{a}_{up} \rrbracket^* = \llbracket \mathbf{a}_{up} \rrbracket \mathbf{H}_E; \quad \llbracket \mathbf{a}_{gp} \rrbracket^* = \llbracket \mathbf{a}_{gp} \rrbracket \mathbf{H}_E. \quad (18a,b)$$

Finally, the solving system is rewritten in compact way with obvious meaning of symbols

$$\mathbf{K} \mathbf{X} + \underbrace{\bar{\mathbf{L}}_u + \bar{\mathbf{L}}_g}_{\bar{\mathbf{L}}} = \mathbf{0} \quad (19)$$

with \mathbf{K} symmetric flexibility matrix of the system, \mathbf{X} vector of nodal unknowns, $\bar{\mathbf{L}}_u$ and $\bar{\mathbf{L}}_g$ load vectors due to $-\bar{\mathbf{U}}$ e $\bar{\mathbf{G}}$ respectively, being $\bar{\mathbf{L}} = \bar{\mathbf{L}}_u + \bar{\mathbf{L}}_g$ the total load vector.

In order to evaluate the coefficients of the equation system the numerical techniques for removing the singularities and the rigid motion strategy have to be employed.

- *Observation about rigid motions*

Let the plate of Fig.2 be subjected to

- a rigid motion of translation obtained as the sum of constant displacement fields \bar{u}_x and \bar{u}_y (Fig.2a),
- a rigid motion of rotation having wideness $\bar{\varphi}$ around any point (Fig.2b),
- a rigid motion of roto-translation obtained as a combination of a) and b).

In all these cases the displacement and normal derivative of the displacement fields are entirely known both in the domain and on the boundary of the plate.

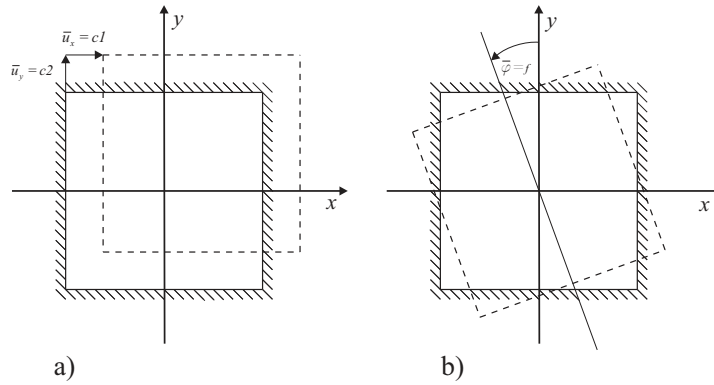


Fig.2 Rigid motions: a) translation, b) rotation.

Particularly

- for the case of rigid motion of translation (Fig.2a)

$$\bar{u}_x = c1, \quad \bar{g}_x = -\frac{\partial \bar{u}_x}{\partial n} = 0$$

$$\bar{u}_y = c2, \quad \bar{g}_y = -\frac{\partial \bar{u}_y}{\partial n} = 0 \quad (20a,b,c,d)$$

with $c1$ and $c2$ being the wideness of the displacements;

- for the case of rigid motion of rotation having width f (Fig.2b)

$$\bar{\varphi} = f \quad (21a)$$

$$\bar{u}_x = -f y \quad \bar{g}_x = -\frac{\partial \bar{u}_x}{\partial n} = f n_y$$

$$\bar{u}_y = f x \quad \bar{g}_y = -\frac{\partial \bar{u}_y}{\partial n} = -f n_x \quad (22b,c,d,e)$$

• *Observations about the load vector as a consequence of the rigid motion*

1) If the solid is subject to a rigid motion of translation (Fig.2a) having assigned values of the displacements $c1$ and $c2$, one has $\bar{\mathbf{U}} \neq \mathbf{0}$ and $\bar{\mathbf{G}} = \mathbf{0}$ but the total load vector has to be $\bar{\mathbf{L}} = \bar{\mathbf{L}}_u + \bar{\mathbf{L}}_g = \mathbf{0}$ with

$$\bar{\mathbf{L}}_u = \begin{bmatrix} (\mathbf{A}_{ut} + \mathbf{C}_{ut}) + \llbracket \mathbf{a}_{up} \rrbracket^* \\ \mathbf{A}_{gt} + \llbracket \mathbf{a}_{gp} \rrbracket^* \end{bmatrix} \cdot \bar{\mathbf{U}} = \begin{bmatrix} \mathbf{0} \\ \mathbf{0} \end{bmatrix} \quad (23)$$

$$\bar{\mathbf{L}}_g = \begin{bmatrix} \mathbf{A}_{ur} \\ \mathbf{A}_{gr} + \mathbf{C}_{gr} \end{bmatrix} \cdot \bar{\mathbf{G}} = \begin{bmatrix} \mathbf{0} \\ \mathbf{0} \end{bmatrix} \quad (24)$$

and as a consequence the solution vector \mathbf{X} will be null.

2) If the solid is subject to a rigid motion of rotation (Fig.2a) having assigned rotation vector $|\bar{\boldsymbol{\varphi}}| = f$, in the generic node i one has

$$\bar{\mathbf{U}}_i = \mathbf{r}_i \times \bar{\boldsymbol{\varphi}} \neq \mathbf{0} \quad \bar{\mathbf{G}}_i = \bar{\boldsymbol{\varphi}} \times \mathbf{n}_i = |\bar{\boldsymbol{\varphi}}| \cdot \mathbf{s}_i \neq \mathbf{0} \quad (25a,b)$$

with \mathbf{r}_i vector distance between the instantaneous center of rotation and the node i , \mathbf{n}_i e \mathbf{s}_i being respectively the unit normal and tangent vectors to the boundary elements on which the node i lies, but the total load vector has to be $\bar{\mathbf{L}} = \bar{\mathbf{L}}_u + \bar{\mathbf{L}}_g = \mathbf{0}$ with

$$\bar{\mathbf{L}}_u = \begin{bmatrix} (\mathbf{A}_{ut} + \mathbf{C}_{ut}) + \llbracket \mathbf{a}_{up} \rrbracket^* \\ \mathbf{A}_{gt} + \llbracket \mathbf{a}_{gp} \rrbracket^* \end{bmatrix} \cdot (-\bar{\mathbf{U}}) \neq \begin{bmatrix} \mathbf{0} \\ \mathbf{0} \end{bmatrix} \quad (26)$$

$$\bar{\mathbf{L}}_g = \begin{bmatrix} \mathbf{A}_{ur} \\ \mathbf{A}_{gr} + \mathbf{C}_{gr} \end{bmatrix} \cdot \bar{\mathbf{G}} \neq \begin{bmatrix} \mathbf{0} \\ \mathbf{0} \end{bmatrix} \quad (27)$$

with $\bar{\mathbf{L}}_u = -\bar{\mathbf{L}}_g$ and as a consequence the solution vector \mathbf{X} will be null.

3) If the solid is subjected to a combination of the rigid motions 1) and 2), the condition $\bar{\mathbf{L}} = \bar{\mathbf{L}}_u + \bar{\mathbf{L}}_g = \mathbf{0}$ has to be always valid and as a consequence $\bar{\mathbf{L}}_u = -\bar{\mathbf{L}}_g$.

For the example considered the vectors $\bar{\mathbf{U}}$, $\bar{\mathbf{U}}_E$ e $\bar{\mathbf{G}}$ are the following, as shown in Fig1c,d.

$$\bar{\mathbf{U}}^T = \left[\left[0 \mid 0 \mid \frac{1}{2} \mid 0 \mid 1 \mid 0 \mid \frac{1}{2} \mid 0 \mid 0 \mid 0 \mid 0 \mid 0 \mid 0 \mid 0 \mid 0 \mid 0 \right] \right]$$

$$\bar{\mathbf{U}}_E^T = \left[\left[0 \mid 0 \mid 1 \mid 0 \mid 0 \mid 0 \mid 0 \mid 0 \mid 0 \right] \right]$$

$$\bar{\mathbf{G}}^T = \left[\left[0 \mid 0 \mid \frac{1}{4} \mid 0 \mid \frac{1}{2} \mid 0 \mid \frac{1}{2} \mid 0 \mid \frac{1}{4} \mid 0 \mid 0 \mid 0 \mid -\frac{1}{2} \mid 0 \mid -\frac{1}{4} \mid 0 \mid 0 \mid 0 \mid 0 \mid 0 \mid -\frac{1}{4} \mid 0 \mid -\frac{1}{2} \mid 0 \right] \right]$$

The results are summarized in Table 2.

In Fig.2 the displacement u_x within the domain along a line placed at $y=0.9$ is shown.

	F_x	F_y		R_x	R_y
a1	-0.011803	0.185476	a1	-0.001659	0.006859
a2	0.123075	0.036725	a2	0.001483	0.024164
b2	0.069233	0.036725	b2	0.001483	0.024164
b3	0.204111	0.185476	b3	0.001659	0.006859
c3	0.608112	0.181202	c3	0.005866	0.001444
c4	0.314798	0.058847	c4	0.002909	0.010441
d4	0.358279	0.058847	d4	-0.002909	0.010441
d5	0.064958	0.181202	d5	-0.005866	0.001444
e5	-0.204111	-0.102985	e5	-0.001659	0.006859
e6	-0.069233	-0.251736	e6	0.001483	0.024164
f6	-0.123075	-0.251736	f6	0.001483	0.024164
f7	0.011803	-0.102985	f7	0.001659	0.006859
g7	-0.064958	-0.011106	g7	0.005866	0.001444
g8	-0.358279	-0.133461	g8	0.002909	0.010441
h8	-0.314798	-0.133461	h8	-0.002909	0.010441
h1	-0.608112	-0.011106	h1	-0.005866	0.001444

Table 2 . Results wedged plate

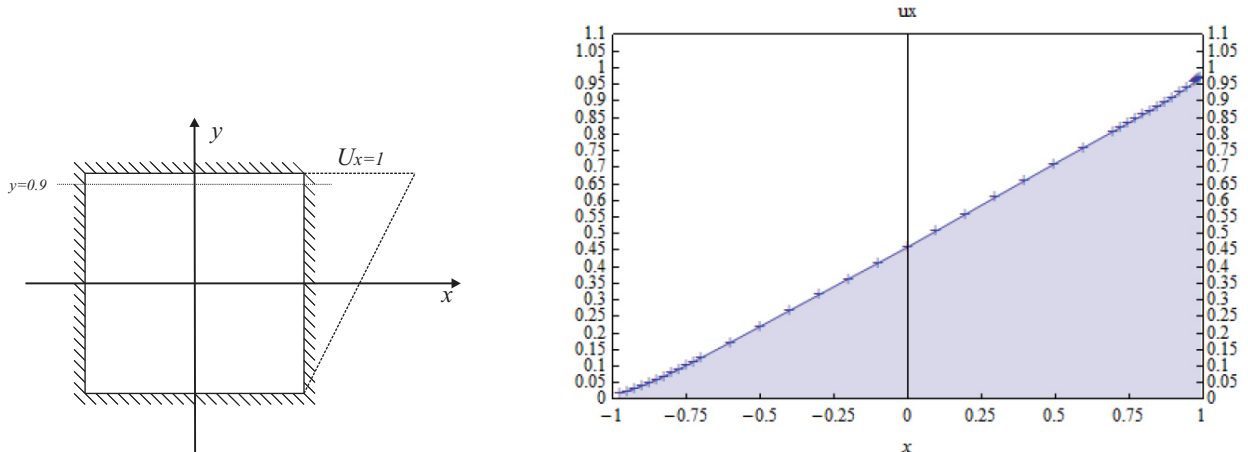


Fig.2 Displacements u_x at $y=0.9$

Conclusions

The table of fundamental solutions for isotropic strain gradient elasticity is similar to an analogous table used within classical boundary element method.

Computational techniques have been pursued in order to eliminate the singularities of order $1/r$, $1/r^2$, in the blocks of the coefficients related to the corners of the solid and new techniques based on the rigid motion strategy have been introduced in order to test the coefficients of the blocks of the solving system. The displacement and internal deformation fields were obtained.

Numerical techniques in order to remove the singularity of higher order like $1/r^3$ and $1/r^4$ are in advanced study.

References.

- [1] Polizzotto, C., Panzeca, T., Terravecchia, S. (2014). "A symmetric Galerkin BEM formulation for a class of gradient elastic materials of Mindlin type. Part I: Theory". In preparation.
- [2] Mindlin, R.D.(1965). "Second gradient of strain and surface tension in linear elasticity". *Int. J. Solids Struct.*, **1**, 417-438.
- [3] Mindlin, R.D., Eshel, N.N., (1968). "On first strain-gradient theories in linear elasticity". *Int. J. Solids Struct.*, **28**, 845-858.
- [4] Wu, C.H. (1992). "Cohesive elasticity and surface phenomena". *Quart. Appl. Math.*, **L(1)**, 73-103.
- [5] Aifantis, E.C. (1992). " On the role of gradients in the localization of deformation and fracture". *Int. J. Eng. Sci.*, **30**, 1279-1299.
- [6] Askes, H., Aifantis, E.C. (2011). " Gradient elasticity in statics and dynamics: An overview of formulations, length scale identification procedures, finite element implementations and new results". *Int. J. Solids Struct.*, **48**, 1962-1990.
- [7] Polyzos, D., Tsepoura, K.G., Tsinopoulos, S.V., Beskos, D.E. (2003). "A boundary element method for solving 2-D and 3-D static gradient elastic problems. Part.I: integral formulation". *Comput. Meth. Appl. Mech. Engng.*, **192**, 2845-2873.
- [8] Karlis, G. F. , Charalambopoulos, A., Polyzos, D. (2010). "An advanced boundary element method for solving 2D and 3D static problems in Mindlin's strain gradient theory of elasticity". *Int. J. Numer. Meth. Engng.*, **83**, 1407-1427.
- [9] Panzeca, T., Cucco, F., Terravecchia S. (2002). "Symmetric Boundary Element Method versus Finite Element Method". *Comp. Meth. Appl. Mech. Engng.*, **191**, 3347-3367.
- [10] Cucco F., Panzeca T., Terravecchia S. (2002). "The program Karnak.sGbem Release 2.1". Palermo University.
- [11] Polizzotto C. (1988) . "An energy approach to the boundary element method. Part.I: elastic solids". *Comput. Meth. Appl. Mech. Engng.*, **69**, 167-184.